

# Predicting the Critical Stress for Initiation of Dynamic Recrystallization

Abbas NAJAFIZADEH<sup>1)</sup> and John J. JONAS<sup>2)</sup>

1) Department of Materials Engineering, Isfahan University of Technology, Isfahan, Iran.

2) Department of Metallurgical Engineering McGill University, 3610 University Street, Montreal, Canada H3A 2B2.

(Received on August 17, 2005; accepted on August 22, 2006)

The critical stress for initiation of dynamic recrystallization (DRX) can be identified from the inflection point on the strain hardening rate ( $\theta = d\sigma/d\varepsilon$ ) versus flow stress ( $\sigma$ ) curve. This kind of curve can be described by an equation that fits the experimental  $\theta$ - $\sigma$  data from zero to the peak stress. Such a curve must have an inflection point and the simplest relation that has such properties is a third order equation.

Hot compression tests were carried out on a 304 H stainless steel over the temperature range 900–1100°C and strain rate range 0.01–1 s<sup>-1</sup> to a strain of 1. An appropriate third order equation was fitted to the strain hardening data. The results show that the critical stress at initiation  $\sigma_c = -B/3A$  where  $A$  and  $B$  are coefficients of the third order equation. It is evident that this value depends on the deformation conditions. The stress-strain curve was then normalized with respect to the peak stress, leading to a normalized value of the critical stress ( $u_c$ ) equal to  $u_c = \sigma_c/\sigma_p = -B'/3A'$ . Here  $A'$  and  $B'$  are coefficients of the normalized third order equation. This value is constant and independent of the deformation conditions.

KEY WORDS: dynamic recrystallization; critical stress; strain hardening rate; 304 H stainless steel; modeling.

## 1. Introduction

Dynamic recrystallization (DRX) is a powerful tool for controlling microstructural evolution and mechanical properties during industrial processing.<sup>1-5)</sup> When this type of softening process is operating, both nucleation as well as growth take place while the strain is being applied.<sup>1,2)</sup>

It is well known that during hot deformation (with a relatively high strain rate) the dislocation density increases while dynamic recovery (DRC) tries to diminish the density. If the rate of dislocation density increase is greater than can be accommodated by DRC, then dynamic recrystallization (DRX) is initiated at a certain point. This applies particularly to low and medium stacking fault energy for fcc metals.

Calculation of the critical condition for the initiation of DRX is of considerable interest for the modeling of industrial processes.<sup>6-9)</sup> It depends on the chemical composition of the material, the grain size prior to deformation, and the deformation conditions (T and  $\varepsilon$ ).<sup>7-10)</sup> Several researchers have proposed mathematical relations to predict the initiation of DRX. For example, M. R. Barnett, G. L. Kelly and P. D. Hodgson<sup>11)</sup> have identified the critical strain for initiation of DRX using the kinetics of static recrystallization (SRX) modified to allow SRX to begin before the end of deformation. This approach defines the critical stress for the initiation of SRX (DRX) during deformation. On the basis of a dislocation density work hardening model, G. Gottstein, M. Frommert, M. Goerdeeler, and N. Schafer<sup>12)</sup> have also predicted the critical strain for initiation of DRX

( $\varepsilon_c$ ).

The onset of DRX can also be identified phenomenologically from the inflection point in the strain hardening rate ( $\theta$ ) versus flow curve ( $\sigma$ ). E. I. Poliak and J. J. Jonas<sup>6-9)</sup> have shown that this corresponds to the appearance of an additional thermodynamic degree of freedom in the system. This signifies that an additional softening mechanism begins to operate (in addition to dynamic recovery). The additional mechanism can be phase transformation, twinning, or precipitate coarsening, but has been identified as dynamic recrystallization in the present case. The critical stress identifies the moment when dynamic recrystallization begins to make a contribution to decreasing the flow stress.

The only difference between this method and the latter method is that we used a third order polynomial equation to fit the strain hardening rate versus flow stress curve. This method has the important practical advantage that it is much easier to use than the previous one, because no fitting of a higher order polynomial is involved.

It was found that the  $\theta$ - $\sigma$  curve can be represented by a third order equation up to the peak stress. Under such conditions, the critical stress for the initiation of DRX is given by the simple relationship  $\sigma_c = -B/3A$ , where  $A$  and  $B$  are two of the four coefficients of the third order equation (see Eq. (1) below).

The values of  $\sigma_c$  obtained in this way depend on the experimental conditions. If instead the normalized stress-strain curve is employed ( $u = \sigma/\sigma_p$  vs.  $w = \varepsilon/\varepsilon_p$ ), the normalized stress for the onset of DRX is given by  $u_c = \sigma_c/\sigma_p = -B'/3A'$ , where  $A'$  and  $B'$  are two of the four

**Table 1.** Chemical composition (wt%) of the 304H stainless steel.

Cr	Ni	Mn	Mo	Cu	C	Si	P	S
17.65	7.91	1.74	0.57	0.32	0.067	0.71	0.026	0.022

coefficients of the normalized third order equation (see Eq. (7) below). According to this approach, the value of  $u_c$  is constant for all the deformation conditions that exhibit DRX behavior in the 304H stainless steel and is given by  $u_c = -B'/3A' = 0.875$ . The validity of these relationships was examined for a 304H stainless steel and good agreement was obtained between the calculated and experimental values of the critical stress.

**2. Experimental Procedure**

The chemical composition of the 304H stainless steel employed in this work is given in **Table 1**. This material was supplied with the form of a hot rolled bar with a diameter of 7.94 mm. Cylindrical samples 7.9 mm in diameter and 11.5 mm in height were prepared with their axes aligned along the rolling direction. One-hit hot compression was carried out on a computer-controlled servo-hydraulic MTS machine equipped with a radiant furnace. The MTS hot compression machine was programmed to operate at constant true strain rate by incremental calculation of the current true strain.

The samples were deformed in an argon atmosphere after the specimens were preheated at 1200°C for 15 min. They were then cooled to the test temperature at 1°C/s and held for 5 min prior to deformation for temperature homogenization purposes. Tests were performed at 900, 950, 1000, 1050 and 1100°C and strain rates of 0.01, 0.1, 0.5 and 1 s<sup>-1</sup>. All samples were deformed to strain of 1. In order to minimize the coefficient of friction during hot compression testing, mica plates covered with boron nitride powder were used for lubrication.

**3. Results and Discussion**

**3.1. Modeling the Stress–Strain Curve**

In the approach of Poliak and Jonas<sup>6-9,13</sup> and N. D. Ryan and H. J. McQueen,<sup>14</sup> the initiation of DRX is associated with the point of inflection in the curve of strain hardening rate  $\theta$  vs. flow stress  $\sigma$ . To plot this kind of curve, it is necessary to find an equation that fits the experimental  $\theta$ – $\sigma$  data from zero until the peak stress. The simplest equation that has an inflection point is:

$$\theta = A\sigma^3 + B\sigma^2 + C\sigma + D \dots \dots \dots (1)$$

where:  $\theta = d\sigma/d\epsilon$  and  $A, B, C,$  and  $D$  are constants for a given set of deformation conditions.

Differentiation of this equation with respect to  $\sigma$  results in:

$$\frac{d\theta}{d\sigma} = 3A\sigma^2 + 2B\sigma + C$$

The minimum point of this second order equation corre-

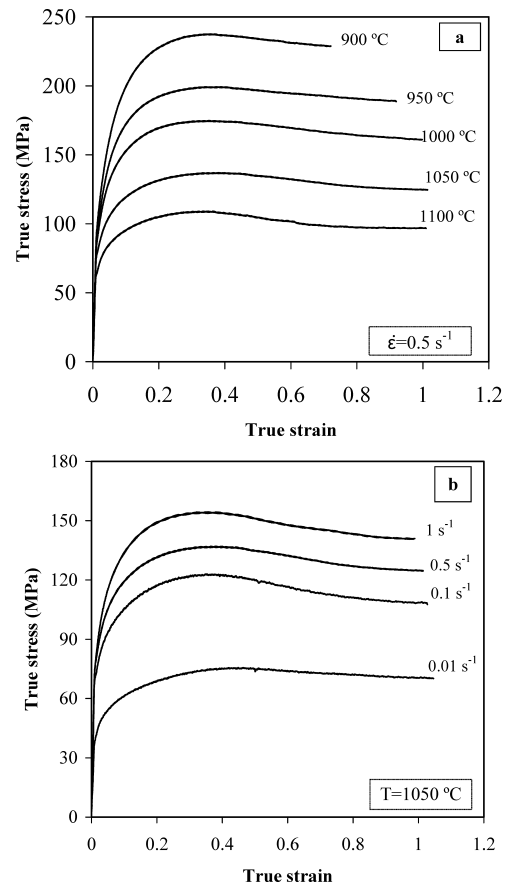


**Fig. 1.** Representative 304H stainless steel flow curves. (a) Various temperatures at a strain rate of 0.5 s<sup>-1</sup>, (b) various strain rates at 1050°C.

sponds to the critical stress, *i.e.*,

$$\frac{d^2\theta}{d\sigma^2} = 0 \Rightarrow 6A\sigma_c + 2B = 0 \Rightarrow \sigma_c = \frac{-B}{3A} \dots \dots \dots (2)$$

• Example

To examine the validity of this equation, a series of hot compression tests were carried out on the 304H stainless steel. Some representative flow curves are presented in **Fig. 1**. These curves exhibit peaks and softening to a steady state, which indicate DRX behavior. The flow stresses depend on the deformation variables, that is the strain rate and temperature. The peak stresses and strains increase as the temperature decreases from 1100 to 900°C as shown in **Fig. 1(a)** as well as with increasing strain rate from 0.01 to 1 s<sup>-1</sup>, see **Fig. 1(b)**. It has been shown that the increasing strain rate makes the attainment of the peak stress more difficult.<sup>7)</sup>

For each condition of deformation, the strain hardening rate was plotted against flow stress and the third order equation that best fit the experimental  $\theta$ – $\sigma$  data from zero to the peak stress was found. For this purpose, fitting was done using the Excel, by choosing the Add Trendline command and then selecting the Third Order Polynomial option. As an example a stress–strain curve determined at 1100°C and a strain rate of 0.1 s<sup>-1</sup> is presented in **Fig. 2**.

The experimental  $\theta$ – $\sigma$  data as well as the third order equation and curve that best fit these data are shown in **Fig. 3**. According to the method of Poliak and Jonas,<sup>6-9)</sup> the next

step required to identify the critical stress ( $\sigma_c$ ) is to plot the derivative of the third order equation *versus* flow stress, see Fig. 4. All the third order equations obtained from this

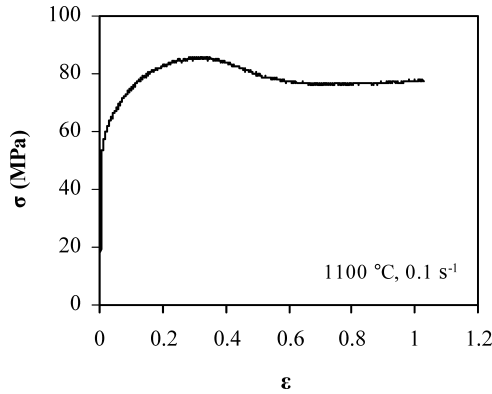


Fig. 2. Hot compression flow curve determined at 1100°C and a strain rate of 0.1 s<sup>-1</sup>.

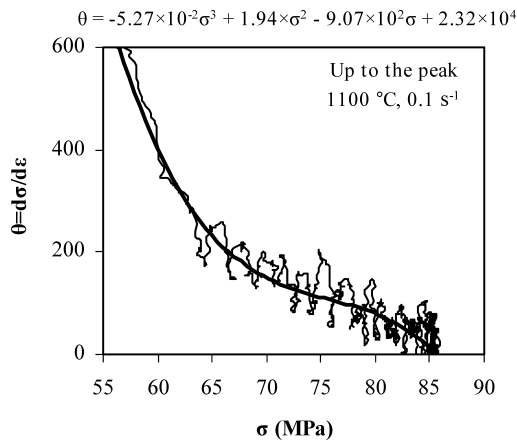


Fig. 3. Strain hardening rate ( $\theta$ ) *versus* flow stress up to a strain of 1 for the experiment of Fig. 2.

study are presented in Table 2.

The relation between the critical stresses calculated using Eq. (2) and the Zener–Hollomon parameter was also studied for the 304 H stainless steel. For this purpose, the activation energy for deformation was derived with the aid of the following expansion of the Zener–Hollomon parameter:

$$Z = \dot{\epsilon} \exp \left[ \frac{Q_{\text{def}}}{RT} \right] = A(\sinh(\alpha\sigma))^n \dots\dots\dots(4)$$

$$Q_{\text{def}} = Rn \left[ \frac{\partial \ln \sinh(\alpha\sigma)}{\partial \ln(1/T)} \right]_{\dot{\epsilon}} \dots\dots\dots(5)$$

Here  $Q_{\text{def}}$  is the apparent activation energy for deformation and  $R$  is the gas constant.<sup>16,17)</sup> The application of these equations to the present data resulted in a mean value of 370 kJ/mol. This quantity is consistent with those measured previously.<sup>5,6,15,18)</sup>

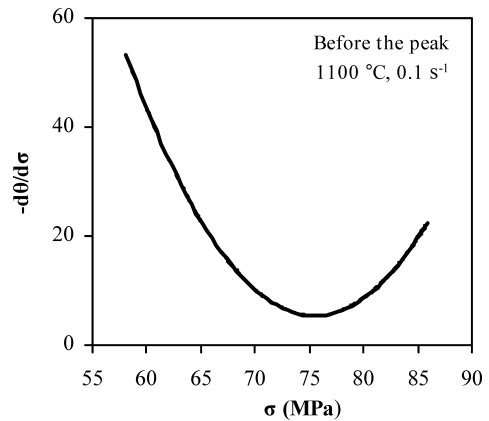


Fig. 4. Stress dependence of the derivative of strain hardening rate ( $\theta$ ) with respect to stress for the flow curve of Fig. 2.

Table 2. Coefficients for strain hardening rate ( $\theta$ ) *versus* stress ( $\sigma$ ) equations,  $T=900\text{--}1100^\circ\text{C}$  and  $\epsilon=0.01\text{--}1\text{ s}^{-1}$ .

Strain rate (s <sup>-1</sup> )	T (°C)	$\theta/\sigma$ relation
0.01	900	$\theta = -1.03 \times 10^{-2} \sigma^3 + 4.64 \sigma^2 - 7.06 \times 10^2 \sigma + 3.62 \times 10^4$
	950	$\theta = -2.21 \times 10^{-2} \sigma^3 + 7.60 \sigma^2 - 8.74 \times 10^2 \sigma + 3.37 \times 10^4$
	1000	$\theta = -3.66 \times 10^{-2} \sigma^3 + 10.3 \sigma^2 - 9.74 \times 10^2 \sigma + 3.06 \times 10^4$
	1050	$\theta = -5.39 \times 10^{-2} \sigma^3 + 10.8 \sigma^2 - 7.24 \times 10^2 \sigma + 1.63 \times 10^4$
	1100	$\theta = -1.38 \times 10^{-1} \sigma^3 + 22.4 \sigma^2 - 1.22 \times 10^3 \sigma + 2.22 \times 10^4$
0.1	900	$\theta = -3.60 \times 10^{-3} \sigma^3 + 2.01 \sigma^2 - 3.78 \times 10^2 \sigma + 2.45 \times 10^4$
	950	$\theta = -1.53 \times 10^{-2} \sigma^3 + 6.03 \sigma^2 - 8.01 \times 10^2 \sigma + 3.60 \times 10^4$
	1000	$\theta = -3.02 \times 10^{-2} \sigma^3 + 8.87 \sigma^2 - 8.73 \times 10^2 \sigma + 2.90 \times 10^4$
	1050	$\theta = -3.69 \times 10^{-2} \sigma^3 + 11.7 \sigma^2 - 1.24 \times 10^3 \sigma + 4.42 \times 10^4$
	1100	$\theta = -5.27 \times 10^{-2} \sigma^3 + 11.9 \sigma^2 - 9.07 \times 10^2 \sigma + 2.32 \times 10^4$
0.5	900	$\theta = -4.00 \times 10^{-2} \sigma^3 + 2.23 \sigma^2 - 4.24 \times 10^2 \sigma + 2.77 \times 10^4$
	950	$\theta = -5.30 \times 10^{-3} \sigma^3 + 2.65 \sigma^2 - 4.48 \times 10^2 \sigma + 2.62 \times 10^4$
	1000	$\theta = -6.70 \times 10^{-3} \sigma^3 + 3.03 \sigma^2 - 4.65 \times 10^2 \sigma + 2.47 \times 10^4$
	1050	$\theta = -1.53 \times 10^{-2} \sigma^3 + 5.54 \sigma^2 - 6.75 \times 10^2 \sigma + 2.79 \times 10^4$
	1100	$\theta = -2.2 \times 10^{-2} \sigma^3 + 6.51 \sigma^2 - 6.52 \times 10^2 \sigma + 2.21 \times 10^4$
1	900	$\theta = -1.70 \times 10^{-3} \sigma^3 + 1.04 \sigma^2 - 2.20 \times 10^2 \sigma + 1.67 \times 10^4$
	950	$\theta = -7.60 \times 10^{-3} \sigma^3 + 3.51 \sigma^2 - 5.52 \times 10^2 \sigma + 2.99 \times 10^4$
	1000	$\theta = -7.10 \times 10^{-3} \sigma^3 + 3.35 \sigma^2 - 5.31 \times 10^2 \sigma + 2.89 \times 10^4$
	1050	$\theta = -1.57 \times 10^{-2} \sigma^3 + 6.09 \sigma^2 - 7.93 \times 10^2 \sigma + 3.49 \times 10^4$
	1100	$\theta = -1.73 \times 10^{-2} \sigma^3 + 5.74 \sigma^2 - 6.42 \times 10^2 \sigma + 2.44 \times 10^4$

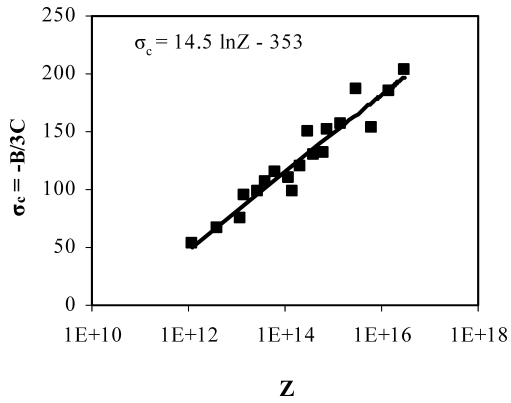


Fig. 5. Dependence of the critical stress for the initiation of DRX on Zener-Hollomon parameter. The measured values are compared with the trend line.

As can be seen from Fig. 5, there is a linear relationship between  $\sigma_c$  and  $\ln Z$ :

$$\sigma_c = 14.6 \ln Z - 354 \dots \dots \dots (6)$$

**3.2. Modeling the Normalized Stress-Strain Curve**

Once normalized stress ( $u = \sigma/\sigma_p$ )-strain ( $w = \epsilon/\epsilon_p$ ) plots have been established, the flow stress at any strain, strain rate and temperature can be calculated from this single curve.<sup>7)</sup> The normalized strain hardening rate ( $\theta_N = du/dw$ )-normalized stress ( $u$ ) plots obtained from such curves have inflection points that identify the point of initiation of DRX in the range of temperature and strain rate of interest. For a given steel, the inflection points in  $\theta_N-u$  plots correspond approximately to identical  $u$ -values, i.e., to approximately constant critical stress ratios  $u_c = \sigma_c/\sigma_p$ . Since the flow curves form a single  $u-w$  plot at various values of  $Z$ , the onset of DRX corresponds to a single point on this plot. Consequently the ratio of the critical strain to the peak strain,  $\epsilon_c/\epsilon_p = w_c$ , is also approximately constant for a given steel deformed within a given temperature and strain rate range.

To identify the critical stress for different conditions of deformation, the normalized stress-strain curve was used. The best fit equation corresponding to these data again had the form:

$$\theta_N = A'u^3 + B'u^2 + C'u + D' \dots \dots \dots (7)$$

In this case, the coefficients of the equation do not depend on the deformation conditions. As mentioned in Sec. 3.1 above, the critical stress for the initiation of DRX can be calculated as follows:

$$\frac{d\theta_N}{du} = 3A'u^2 + 2B'u + C' \dots \dots \dots (8)$$

And a second derivation of this equation results in:

$$\frac{d^2\theta_N}{du^2} = 6A'u_c + 2B' = 0 \Rightarrow u_c = \frac{-B'}{3A'} \dots \dots \dots (9)$$

Using this relationship, the critical stress for any set of deformation conditions can be calculated solely using  $\sigma_p$  for this condition. This approach also helps to explain the

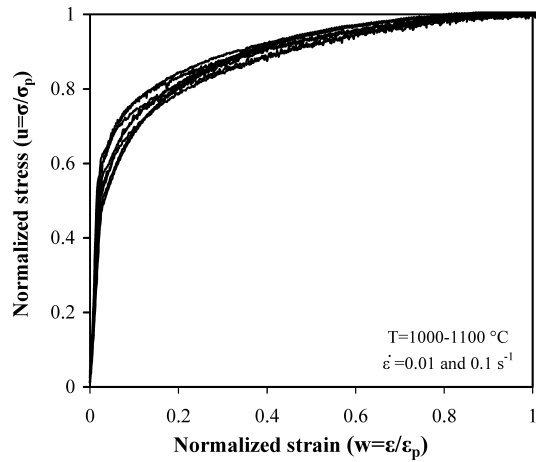


Fig. 6. Normalized stress-strain curves obtained under different conditions of deformation.

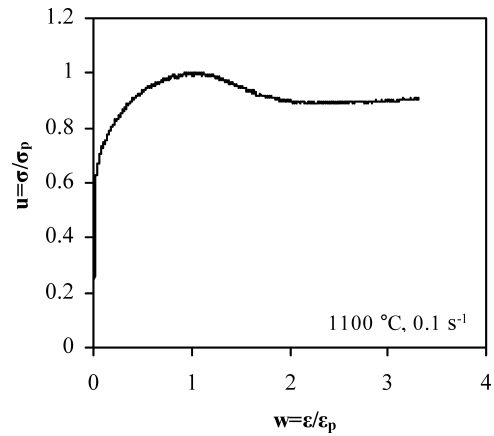


Fig. 7. Normalized stress-strain curve pertaining to a deformation temperature of 1100°C and a strain rate of 0.1 s<sup>-1</sup>.

constancy of the  $\sigma_c/\sigma_p$  ratio.

• Example

Some normalized stress-strain curves of the present 304H stainless steel deformed under different conditions are illustrated in Fig. 6. As can be seen, there are small discrepancies that arise from a weak dependence of the curves on the value of  $Z$ . This source of error can be reduced by deriving 3 normalized curves pertaining to three different sets of deformation conditions and then averaging for  $u_c$  and also for the coefficients of Eqs. (7) and (9).

One of the normalized stress-strain curves determined at 1100°C and a strain rate of 0.1 s<sup>-1</sup> is presented in Fig. 7. The corresponding normalized strain hardening rate versus flow stress curve is illustrated in Fig. 8. The third order equation that best fits these data is:

$$\theta_N = -115.2u^3 + 302.2u^2 - 265.8u + 78.82 \dots \dots \dots (10)$$

The derivative of the normalized strain rate hardening versus normalized stress curve is depicted in Fig. 9. The minimum point in this curve represents the critical stress for the initiation of DRX. As mentioned above, the value of  $u_c$  for the material studied in the present work can be determined from the second derivative of Eq. (10):

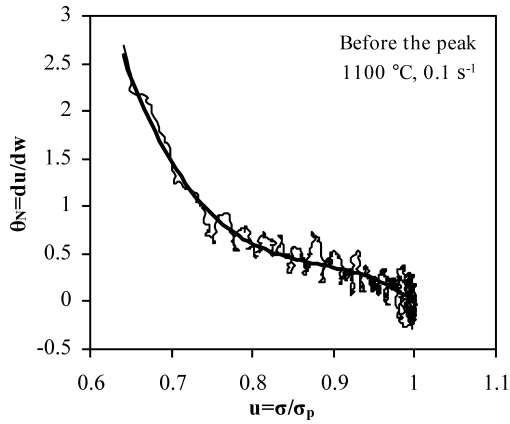


Fig. 8. Normalized strain hardening rate versus normalized stress for the flow curve of Fig. 7.

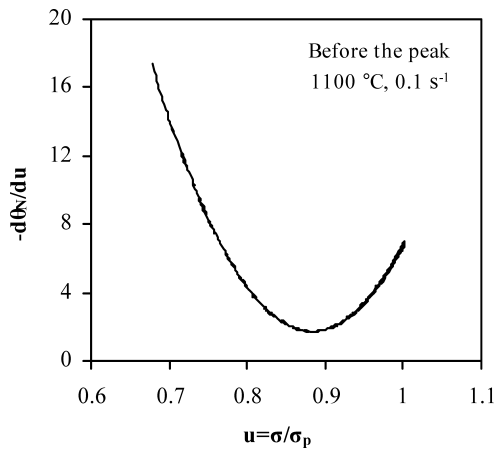


Fig. 9. Normalized stress dependence of the derivative of the normalized strain hardening rate illustrated in Fig. 8.

$$u_c = \frac{-302.2}{3 \times 115.2} = 0.875 \dots\dots\dots(11)$$

This value is expected to be constant under all conditions of deformation where DRX is taking place. This hypothesis can be assessed by plotting the measured values of  $\sigma_c$  versus those calculated from Eq. (11). Such a comparison is presented in Fig. 10. As can be seen, there is reasonably good agreement between these two sets of values.

The value of  $u_c$  derived in Eq. (11) should be independent of the deformation conditions. The relative lack of dependence of  $u_c$  on  $Z$  is illustrated in Fig. 11.

It should be mentioned here that the  $\theta_N-u$  curve can be best fitted not only using 3rd but also 4th, 5th, and higher order equations. The critical values of the normalized stress ( $u_c$ ) obtained from the second derivatives of these equations were 0.865 and 0.860 for the 4th and 5th order equations, respectively. As the difference between the 3rd and 5th order values is less than 2%, the simplifications arising from using the 3rd order method probably justify this approach.

4. Conclusions

The principal conclusions that can be drawn from the present work are the following:

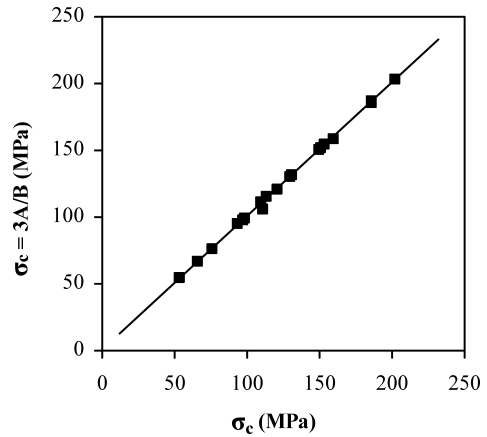


Fig. 10. Critical stresses for the initiation of DRX ( $\sigma_c$ ). Here the measured values (horizontal axis) are compared with those estimated using the relation  $\sigma = 0.875\sigma_p$  (vertical axis).

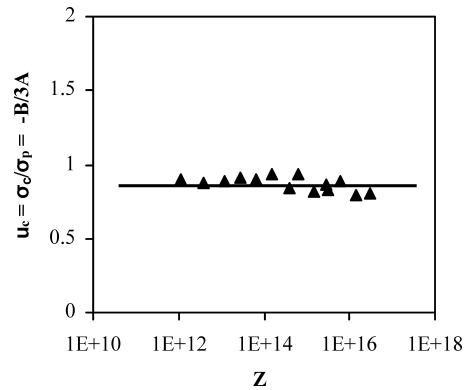


Fig. 11. Z-independence of the critical stress for the initiation of DRX.

- (1) When DRX is occurring, the strain hardening rate versus stress curve can be represented by a third order equation (until the peak stress).
- (2) The critical stress for the initiation of DRX can be calculated by setting the second derivative of such an equation to zero.
- (3) The normalized critical stress for the initiation of DRX ( $u_c$ ) calculated from the normalized strain hardening rate versus normalized stress is approximately constant and independent of the deformation conditions.
- (4) The critical value  $u_c$  for the 304H stainless steel is 0.875.

Acknowledgements

One of the authors (A. Najafizadeh) expresses his thanks to the Isfahan University of Technology for granting a period of sabbatical leave during which this work was carried out.

REFERENCES

- 1) J. J. Jonas: *Mater. Sci. Eng. A*, **A184** (1994), 155.
- 2) R. D. Doherty, D. A. Hughes, F. J. Humphreys, J. J. Jonas, D. J. Jensen, M. E. Kassner, W. E. King, T. R. McNelley, H. J. McQueen and A. D. Rollett: *Mater. Sci. Eng. A*, **A238** (1997), 219.
- 3) H. J. McQueen, S. Yue, N. D. Ryan and E. Fry: *Mater. Process. Technol.*, **53** (1995) 293.
- 4) G. R. Stewart, J. J. Jonas and F. Montheillet: *ISIJ Int.*, **44**, (2004),

- No. 9, 1581.
- 5) F. Montheillet and J. J. Jonas: *Encycl. Appl. Phys.*, **16** (1996), 205.
  - 6) E. I. Poliak and J. J. Jonas: *Acta Mater.*, **44** (1996), No. 1, 127.
  - 7) E. I. Poliak and J. J. Jonas: *ISIJ Int.*, **43** (2003), No. 5, 684.
  - 8) E. I. Poliak and J. J. Jonas: *ISIJ Int.*, **43** (2003), No. 5, 692.
  - 9) J. J. Jonas and E. I. Poliak: *Mater. Sci. Forum*, **426–432** (2003), 57.
  - 10) H. J. McQueen: *Mater. Sci. Eng. A*, **A101** (1998), 149.
  - 11) M. R. Barnett, G. L. Kelly and P. D. Hodgson: *Scr. Mater.*, **43** (2000), 365.
  - 12) G. Gottstein, M. Frommert, M. Goerdeeler and N. Schafer: *Mater. Sci. Eng. A*, **A387–389** (2004), 604.
  - 13) E. I. Poliak and J. J. Jonas: *ISIJ Int.*, **44** (2004), No. 11, 1874.
  - 14) N. D. Ryan and H. J. McQueen: *Can. Metall. Q.*, **29** (1990), 147.
  - 15) M. E. Wahabi, J. M. Cabrera and J. M. Prado: *Mater. Sci. Eng. A*, **A343** (2003), 116.
  - 16) S. F. Medina and C. A. Hernandez: *Acta Mater.*, **44** (1996), 137.
  - 17) S. F. Medina and C. A. Hernandez: *Acta Mater.*, **44** (1996), 1.
  - 18) S.-I. Kim and Y.-C. Yoo: *Mater. Sci. Eng. A*, **A311** (2001), 108.